

Received September 22, 2020, accepted October 7, 2020, date of publication October 20, 2020, date of current version October 28, 2020.

Digital Object Identifier 10.1109/ACCESS.2020.3032449

A Nonlinear Sliding Mode Controller of Serial Robot Manipulators With Two-Level Gain-Learning Ability

DANG XUAN BA¹ , (Member, IEEE), AND JOONBUM BAE² , (Member, IEEE)

¹Department of Automatic Control, HCMC University of Technology and Education (HCMUTE), Ho Chi Minh City 71307, Vietnam

²Department of Mechanical Engineering, Ulsan National Institute of Science and Technology (UNIST), Ulsan 44919, South Korea

Corresponding author: Dang Xuan Ba (badx@hcmute.edu.vn)

This work was supported by the Ho Chi Minh City University of Technology and Education, Vietnam, under Grant T2020-17TD.

ABSTRACT This article presents a learning robust controller for high-quality position tracking control of robot manipulators. A basic time-delay estimator is adopted to effectively approximate the system dynamics. A low-level control layer is structured from the control error as an indirect control objective using new nonlinear sliding-mode synthesize. To realize the control objective with desired transient time, a robust sliding mode control signal is then designed based on the obtained estimation results in a high-level control layer. To promptly suppress unpredictable disturbances, adaptation ability is integrated to the controller using two-level gain-learning laws. Reaching gains and sliding gain are automatically tuned for asymptotic control performance. Effectiveness of the designed controller is concretely confirmed by the Lyapunov-based stability criterion, comparative simulations, and real-time experiments.

INDEX TERMS Manipulators, gain adaptive control, nonlinear sliding mode, position control, robust adaptive control, time-delay estimation.


I. INTRODUCTION

Robots have been playing a key role in automation and are integral parts of developed industries such as heavy industries, mining, automobiles, construction, and consumer goods [1], [2]. Robots will continue to be the cornerstone of upcoming industrial revolutions, thanks to the ability of replacing humans perform production tasks and other activities with very high efficiency [3]–[5]. To accomplish such tasks, the robots need good controllers that can provide high-precision control and fast responses [3], [6]. However, nonlinear uncertain deviations and complicated working environment are impediments in exhibiting excellent robotic controllers [7]–[9].

To represent the system behaviors, mathematical-based methods have been applied using Newton-Euler analyses, Lagrange methods, or virtual decomposition principles [9], [10]. Although general forms of the system dynamics could be derived, it is not easy to determine all detailed parameters due to the specific robot designs, and unknown disturbances

[11], [12]. The mathematical-based problem could be tackled by fuzzy-logic or neural-network-based approaches [7], [8], [13]. The system behaviors could be accurately estimated by the soft computation methods but tuning a vast number of weighted parameters could reduce their applicability in real-life missions [7], [14]. As a result, a simpler dynamical-approximation method, naming time-delay estimation (TDE), has been recently developed to fill up such the gap [15], [16]. By using past measuring acceleration and control inputs, the current total dynamics could be computed based on selected nominal input gains [6], [17]. Effectiveness of the TDE methods resulted in a massive number of publications [18], [19].

To realize the control objective by dealing with modeling errors and disturbances, robust nonlinear controllers have been studied in backstepping, sliding-mode control (SMC), or inverse model control schemes [20]–[25]. Indeed, the total disturbances in the system dynamics could be rejected by an integral-type control design [21], or well estimated and then eliminated by a disturbance-observer control framework [23], [26]. Asymptotic control results were obtained using such controllers but employing with fixed

The associate editor coordinating the review of this manuscript and approving it for publication was Yangmin Li .

control gains might not uphold the excellent performances in various working states [28], [29].

As a sequence, gain-adaptive model-based controllers have been progressively researched based on sliding-mode schemes for robotic systems [27]–[30]. For attenuating a high-frequency switching problem, the robust gains were allowed varying with respect to the controlled sliding surface under a learning law [27]: the gain would dramatically increase to force the surface into a given bound and relaxed thereafter. Since the gain was coupled with a discontinuous function, its so-large value, even in a short time, could lead to a danger of the system hardware. Other learning rules were applied to the nominal input gain matrix of the TD estimation [30], [31] or focused on the driving gains [28] for minimizing the control errors. Various versions of the sliding-mode control (SMC) policies associated with robust-gain estimation or disturbance observers were successfully applied to mechatronic systems [32], [33]. Flexibility of the controller operation has been improved but the terminal or super-twisting SMC schemes provided excellent control performances only in small-attraction regions around the origin. Their transient-convergence rates of reaching and sliding phases were also slower than those of the linear SMC [34], [35]. Furthermore, ones still need to tune the sliding gains for different working conditions.

Another aspect in gain-learning designs has been discovered using intelligent approaches. The best gains were solved for the best control performance using backtracking search algorithms applied on fuzzy logic background [36], or for satisfying an optimal problem [37]. Their effect was confirmed by simulation and experimental results, but gain-variation dynamics need to be further considered.

A parallel series of the gain-learning direction is of the backstepping approaches. The control error was well suppressed using PID control design in which the control gains were activated by a backstepping-based damping function [38]. Facilitation of the controller was exhibited but outstanding infinite-time control performances were not confirmed. To provide an asymptotic control result with automatically tunable gains, a flexible robust backstepping controller was exploited [39]. Variation of all control gains were automatically activated for an asymptotic control performance. However, the convergence rate of the control system did not gratify given constraints.

For high-accuracy control quality both in transient and steady-state phases, prescribed-performance (PP) transformation indexes were employed in nonlinear control structures [13], [40], [41]. The PP controllers could drive the control objective into a small bound around zero with a desired rate [42], [43]. The great feature is hold if the initial conditions of the control error are inside a known range. With few unpredictable cases where the error is out of the desired range, the system might be instable. Furthermore, the original PP controllers do not provide an asymptotic control performance.

In this study, we propose a novel adaptive robust sliding mode controller for position tracking control of robot

manipulators ensuring a prescribed asymptotic performance. A conventional TDE is employed to eliminate influence of the system dynamics on the control performance. By extending results of the previous work [35], a new sliding mode manifold is designed by synthesizing various information of the control error as an indirect control objective in a low-level control layer. A basic sliding-mode control rule is adopted as a high-level control layer to stabilize the manifold around the origin using driving and robust control signals. A two-level gain-learning mechanism is designed to automatically tune the driving, robust and sliding gains of both the two layers. The adaptation laws could promptly suppress unpredictable disturbances and efficiently distribute the robustness burden of the closed-loop system to other potential terms. Key contributions of the proposed controller are highlight as follows:

- 1) The sliding manifold, which is a nonlinear combination of the respect control errors, could speed up the transient-convergence rate in sliding phases. The learning law of the sliding gain is proposed in the low-level control layer for improving the state-state control accuracy.
- 2) Inspired from previous works [35], [39], learning laws of the high-level control layer are modified for improving the reaching control performance. An adaptation mechanism of the driving and robust gains is designed to separately excite for large and small ranges of the sliding surfaces, respectively.
- 3) Its effectiveness is theoretically proven using Lyapunov-based analyses.
- 4) Feasibility and feasibility of the proposed controller are intensively verified by simulations and real-time experimental results.

The remainder of this article is organized as follows. Section II describes the system modeling and control objective. The robust controller with full learning ability is designed in Section III. The simulation results on a two-link robot and real-time experiments on the first joint of a 6DOF robot are discussed in Section IV. The paper is then concluded in Section V.

Notation: \bullet_{\min} , and \bullet_{\max} are the minimum and maximum values of \bullet , respectively, $\hat{\bullet}$, $\bar{\bullet}$, $\check{\bullet} \triangleq \bullet - \bar{\bullet}$ present the estimation, nominal value and variation of \bullet , respectively, $\Delta_{\bullet} \triangleq |\bullet|_{\max}$ denotes the bound of \bullet , $\lambda[\bullet]$ is an eigen value of the matrix \bullet .

II. SYSTEM MODELING AND PROBLEM STATEMENTS

Behaviors of a serial n -link robot are described using the following dynamics:

$$\mathbf{M}[\theta] \ddot{\theta} + \mathbf{C}[\theta, \dot{\theta}] \dot{\theta} + \mathbf{g}[\theta] + \mathbf{f}[\dot{\theta}] + \tau_d = \tau \quad (1)$$

where θ , $\dot{\theta}$, $\ddot{\theta} \in \mathbb{R}^n$ are vectors of joint positions, velocities, and accelerations, respectively, $\mathbf{M}[\theta] \in \mathbb{R}^{n \times n}$ is a positive-definite mass matrix, $\tau \in \mathbb{R}^n$ is a control input vector, $\mathbf{C}[\theta, \dot{\theta}] \dot{\theta}$, $\mathbf{g}[\theta]$, $\mathbf{f}[\dot{\theta}]$, $\tau_d \in \mathbb{R}^n$ is a Coriolis-Centripetal vector, gravitation, friction, and disturbance torques, respectively.

The general dynamics of the robot could be rewritten as in (2) by eliminating the mass matrix $\mathbf{M}[\theta]$ in the left side of (1).

$$\ddot{\theta} = \mathbf{v}[\theta] + \bar{\mathbf{M}}^{-1}[\theta] \tau \quad (2)$$

where $\mathbf{v} \triangleq -\mathbf{M}^{-1}(\mathbf{C}\dot{\mathbf{q}} + \mathbf{g} + \mathbf{f} + \tau_d - \tau) - \bar{\mathbf{M}}^{-1}\tau \in \mathbb{R}^n$ is a total internal dynamical vector which is combined from the mass variation, Coriolis/Centripetal, gravity, friction, disturbances, modeling errors and unmodeled terms.

Let define a tracking error of the system output (θ) and a constrained reference profile (θ_d) as a control objective. The goal of this article is to control the error converge to zero under a desired rate. However, the presence of the nonlinear dynamics, uncertainties, modeling errors and unpredictable disturbances could degrade the control performance of the closed-loop system in complex working environments.

III. TWO-LEVEL GAIN-LEARNING NONLINEAR SLIDING MODE CONTROLLER

In the following, a robust position controller is developed using a time-delay estimator and nonlinear sliding manifold synthesize. Gain-learning laws are studied to effectively treat the lumped disturbance for a desired control quality.

A. ROBUST NONLINEAR SLIDING MODE CONTROL

Assume that the desired trajectory (θ_d) is a known, bounded and twice continuously differentiable signal, and also assume that the system outputs (θ , $\dot{\theta}$) are measurable. To achieve a high control accuracy by abating unexpected effect of the systematic certainties and disturbances, a TDE control term and robust driving functionality are employed with the following design.

The position control error is mathematically presented as

$$\mathbf{e} = \theta - \theta_d \quad (3)$$

A nonlinear sliding manifold is then synthesized as an indirect control objective of the studied system in a low-level control layer:

$$\mathbf{s} = \dot{\mathbf{e}} + \mathbf{K}_0(\mathbf{e} + \mathbf{e}^{p_1/q_1}) \quad (4)$$

where $\mathbf{K}_0 = \text{diag}[\mathbf{k}_0] = \text{diag}[[k_{01}; \dots; k_{0n}]]$ is a positive-definite diagonal sliding gain matrix, and p_1, q_1 are positive odd constants satisfying a constraint of ($q_1 < p_1 < 2q_1$).

Differentiating the manifold (4) with respect to time and yielding the dynamics (2), we have

$$\dot{\mathbf{s}} = \mathbf{v} + \mathbf{M}^{-1}\tau - \ddot{\theta}_d + \mathbf{K}_0 \left(\mathbf{I} + \frac{p_1}{q_1} \text{diag} \left[\mathbf{e}^{(p_1-q_1)/q_1} \right] \right) \dot{\mathbf{e}} \quad (5)$$

From the system (5), the final control signal can be simply designed to stabilize the tracking error to zero in infinite time using the following structure:

$$\tau = \bar{\mathbf{M}}(\tau_{\text{MOD}} + \tau_{\text{DRI}} + \tau_{\text{ROB}}) \quad (6)$$

The detailed control signals ($\tau_{\text{MOD}}, \tau_{\text{DRI}}, \tau_{\text{ROB}}$) are explained hereafter. τ_{MOD} is a model-compensation signal

that is used to eliminate the internal dynamics (\mathbf{v}) and other terms of the surface dynamics (5). Hence, the signal is formed as follows:

$$\tau_{\text{MOD}} = -\hat{\mathbf{v}} + \ddot{\theta}_d - \mathbf{K}_0 \left(\mathbf{I} + \frac{p_1}{q_1} \text{diag} \left[\mathbf{e}^{(p_1-q_1)/q_1} \right] \right) \dot{\mathbf{e}} \quad (7)$$

Estimation of the internal dynamics (\mathbf{v}) is obtained by using the simple time-delay estimator [15], [27]:

$$\hat{\mathbf{v}} = \ddot{\theta}_{t-T_s} - \bar{\mathbf{M}}^{-1}\tau_{t-T_s} \quad (8)$$

where ($t - T_s$) is a time-delay value, and T_s is the sampling time.

By applying the designed control signal (6)-(7), the dynamics (5) of the sliding manifold are reformed as

$$\dot{\mathbf{s}} = \delta + \tau_{\text{DRI}} + \tau_{\text{ROB}} \quad (9)$$

where $\delta \triangleq [\delta_1; \delta_2; \dots; \delta_n] = -\tilde{\mathbf{v}} \in \mathbb{R}^n$ is an estimation-error vector.

The second term τ_{DRI} acts as a driving signal that forces the sliding manifold from everywhere back to around zero. Thus, it is designed as

$$\tau_{\text{DRI}} = -\mathbf{K}_1 \mathbf{s} \quad (10)$$

where $\mathbf{K}_1 = \text{diag}[\mathbf{k}_1] = \text{diag}[[k_{11}; \dots; k_{1n}]]$ is a positive-definite diagonal driving gain matrix.

The last signal τ_{ROB} is a robust control term that is used to suppress the estimation error (δ). The signal is designed as follows:

$$\tau_{\text{ROB}} = -\mathbf{K}_2 \text{sgn}[\mathbf{s}] \quad (11)$$

where $\mathbf{K}_2 = \text{diag}[\mathbf{k}_2] = \text{diag}[[k_{21}; \dots; k_{2n}]]$ is a positive-definite robust gain which should be greater than the bound of the overall error:

$$k_{2i|i=1..n} \geq \Delta_{|\delta_i|} \quad (12)$$

Remark 1: As noted in the TDE theory [17], [18], [27], [30], the nominal inertial matrix is recommended to be satisfied the following condition:

$$\left\| \mathbf{I} - \mathbf{M}^{-1}\bar{\mathbf{M}} \right\|_2 < 1 \quad (13)$$

In fact, the nominal value $\bar{\mathbf{M}}$ could be chosen to be small enough.

Remark 2: For accomplishing the reaching phase, the robust gain (\mathbf{K}_2) should be selected to be large enough or as least comply with the constraint (12). Nevertheless, employing very-big values of the gain would create chattering phenomena that could reduce lifetime of used actuators [27], [28].

Remark 3: The transient control rate of the reaching phase could be speed up by the large driving gain (\mathbf{K}_1) which could yet increase the overall estimation error (δ) [18], [44], [45].

Remark 4: As noted in [35], the transient control quality of the sliding phase is improved by employing the nonlinear sliding manifold (4). However, this effect is diminished when the control errors approach to the origin.

Remark 5: the steady-state control accuracy could be increased with the large gain (\mathbf{K}_0) [4], [5], [28]. Notwithstanding, from the control signal (7), the sliding gain (\mathbf{K}_0) is coupled with a time-derivative term. Hence, employing such the so-big values in cases of numerical velocity computation might amplify the noise effect. Generally, the proposed TDE sliding mode design could provide an excellent control result with the proper control gains regardless of the presence of the disturbances. Tuning such the perfect gains for various working conditions in the real-time control is not a trivial work.

TABLE 1. Detailed parameters of the simulation model.

Description	Parameters	Values	Unit
Link length l	l_1, l_2	0.2, 0.1	m
Gravitational Accel	g	9.81	m/s ²
Friction coefficient	a_1, a_2	50, 50	N.s
Mass of links	m_1, m_2	10, 5	kg

B. TWO-LEVEL GAIN ADAPTATION

To support the gain-selection effort for the users, an automatic gain-tuning feature is integrated into the robust control design.

The driving and robust control gains (\mathbf{k}_1 and \mathbf{k}_2) in the high-level control layer are separated into two terms: nominal gains ($\bar{\mathbf{k}}_1$ and $\bar{\mathbf{k}}_2$) and variation gains ($\check{\mathbf{k}}_1$ and $\check{\mathbf{k}}_2$). The nominal values play a groundwork role in ensuring the stability and the convergence rate of the reaching phase. Influence of unpredictable disturbances on the reaching control performance is overcome by variation gains, which are tuned using the following mechanism:

$$\begin{cases} \dot{\check{\mathbf{k}}}_1 = -\text{diag}[\eta_1] \check{\mathbf{k}}_1 + \Xi_s s^{(p_2+q_2)/q_2} \\ \dot{\check{\mathbf{k}}}_2 = -\text{diag}[\eta_2] \check{\mathbf{k}}_2 + \Xi_s |s|^{p_2/q_2} \end{cases} \quad (14)$$

where Ξ_s , $\text{diag}[\eta_1]$ and $\text{diag}[\eta_2]$ are positive-definite diagonal constant matrices, p_2, q_2 are positive odd constants satisfying a constraint of ($0 < p_2 < q_2$).

The driving and robust gains only force the sliding manifold (\mathbf{s}) back to zero in infinite time in the reaching phase. For promptly driving the control error to zero in the sliding phase, in the low-level control layer, a new learning law is proposed for the sliding gain (\mathbf{k}_0). The gain is designed as follows:

$$\mathbf{k}_0 = \bar{\mathbf{k}}_0 + \check{\mathbf{k}}_0^2 \quad (15)$$

Here, the selected nominal gain ($\bar{\mathbf{k}}_0$) is positive, while the variation gain is updating using the mechanism (16).

$$\dot{\check{\mathbf{k}}}_0 = -\text{diag}[\eta_0] \check{\mathbf{k}}_0 + \Xi_e e^{(p_1-q_1)/q_1} - \Xi_0 |s| \quad (16)$$

where Ξ_e, Ξ_0 and $\text{diag}[\eta_0]$ are positive-definite diagonal constant matrices.

Note that, in cases of using the varying sliding gain, the model-compensation control signal (7) is modified as follows:

$$\begin{aligned} \tau_{\text{MOD}} &= -\hat{\mathbf{v}} + \ddot{\boldsymbol{\theta}}_d - \mathbf{K}_0 \left(\mathbf{I} + \frac{p_1}{q_1} \text{diag} \left[\mathbf{e}^{(p_1-q_1)/q_1} \right] \right) \dot{\mathbf{e}} \\ &\quad + 2\check{\mathbf{K}}_0 \left(\text{diag}[\eta_0] \check{\mathbf{K}}_0 + \Xi_0 \text{diag} [|s|] \right) \mathbf{e} \\ &\quad - 2\check{\mathbf{K}}_0 \left(\left(\Xi_e - \text{diag}[\eta_0] \check{\mathbf{K}}_0 - \Xi_0 \text{diag} [|s|] \right) \mathbf{e}^{p_1/q_1} \right. \\ &\quad \left. + \Xi_e e^{(2p_1-q_1)/q_1} \right) \\ &\quad - \left(\text{diag}[\mathbf{e}] \mathbf{K}_0 - \text{diag}[\mathbf{e}^2] \check{\mathbf{K}}_0 \Xi_0 \text{diag} [\text{sgn} |s|] \right) \\ &\quad \times |s|^{(q_2-p_2)/q_2} \end{aligned} \quad (17)$$

C. STABILITY ANALYSIS

Effectiveness of the closed-loop system is achieved by the following statements.

Theorem 1:

If applying the robust nonlinear sliding mode design (6)-(11) and (17) with gain-adaptation laws (14)-(16) to a nonlinear uncertain system (2), for a predefined nominal robust gain ($\bar{\mathbf{k}}_2$) and proper excitation coefficient ($\Xi_e \leq \bar{\mathbf{K}}_0$), the following properties hold:

- If the estimation error (δ) satisfies the constraint (12), the closed-loop system asymptotically converges to the origin under a certain exponential rate of $\sigma = 2 \min [\bar{k}_1 \min, \eta_1 \min, \eta_2 \min, \bar{k}_0 \min]$.
- Otherwise, the control error converges to the following bound under an exponential rate of $\sigma = 2 \min \left[(\bar{k}_1 \min - \frac{p_2}{p_2+q_2}), \eta_1 \min, \eta_2 \min, \bar{k}_0 \min \right]$ with ($\bar{\mathbf{k}}_1 \min > 1$):

$$\|\mathbf{e}\| \rightarrow \sqrt{\frac{\frac{2}{\sigma \lambda_{\max} [\Xi_s \mathbf{K}_0]} \frac{q_2}{p_2+q_2} \text{trace} \left[\Xi_s (\Delta_\delta - \bar{\mathbf{K}}_2)^{(p_2+q_2)/q_2} \right]}{\frac{1}{\lambda_{\max} [\Xi_s \mathbf{K}_0]} \left((s^{p_2/q_2})^T \Xi_s s + \sum_{i=1}^2 (\check{\mathbf{k}}_i^T \check{\mathbf{k}}_i) \right)}} \quad (18)$$

Theorem 1 is proven in *Appendix A*.

Remark 6: The estimation error (δ) reflexes the change of the internal disturbances [17], [38]. The first statement of Theorem 1 indicates that the closed-loop system would be asymptotically stable for static loads or low-frequency tracking profiles, and the nominal robust gain ($\bar{\mathbf{k}}_0$ and $\bar{\mathbf{k}}_2$) could be chosen with proper values for desired convergence rates.

Remark 7: The bound (18) and the learn rule (16) reveal that the high-level variation gains ($\check{\mathbf{k}}_1, \check{\mathbf{k}}_2$) work as active-disturbance-compensation terms in the reaching phase, while the sliding-gain variation ($\check{\mathbf{k}}_0$) would strongly activate in the sliding phase or as the sliding manifold is inside a certain range. Different from previous works [35], [39], the learning law (14) is designed such that the variation gains ($\check{\mathbf{k}}_1, \check{\mathbf{k}}_2$)

TABLE 2. Selected parameters of the controllers.

Description	Parameters	Values
<i>RLTDE Controller [27]</i>		
Nominal mass matrix	$\bar{\mathbf{M}}$	$0.0\mathbf{I}_2$
Driving and robust gains	$\mathbf{K}_{c1}, \mathbf{K}_{c2}$	$60\mathbf{I}_2, 10\mathbf{I}_2$
Sliding gain	\mathbf{K}_{c0}	$10\mathbf{I}_2$
Steady-state sliding surface	χ	0.015
Learning rates	φ, α	$\text{diag}[4000; 3000]$, $\text{diag}[0.6; 1.57]$
<i>PPPD Controller [48]</i>		
Initial bounds	ρ_{10}, ρ_{20}	60, 60 (deg)
Steady-state bounds	$\rho_{1\infty}, \rho_{2\infty}$	0.287, 0.287 (deg)
Convergence rate	γ	5
Undershoot	κ	1
Control gains	$\mathbf{K}_v, \mathbf{K}_p$, and \mathbf{K}_e	$5\mathbf{I}_2, 100\mathbf{I}_2$, and $\text{diag}[5; 1]$
<i>MLTDE Controller [31]</i>		
Lower bound of nominal mass matrix	$\bar{\mathbf{M}}^-$	$0.0\mathbf{I}_2$
Sliding gain	\mathbf{K}_{c0}	$15\mathbf{I}_2$
Learning rates	α, δ	$\text{diag}[0.005; 0.001]$, $\text{diag}[10^{-5}; 10^{-5}]$
<i>Proposed Controller</i>		
Nominal mass matrix	$\bar{\mathbf{M}}$	$0.0\mathbf{I}_2$
Nominal sliding, driving, and robust gains	$\bar{\mathbf{K}}_{c0}, \bar{\mathbf{K}}_{c1}$, and $\bar{\mathbf{K}}_{c2}$	$5\mathbf{I}_2, 30\mathbf{I}_2, 5\mathbf{I}_2$
Learning rates	η_0, η_1 , and η_2	$[0.02; 0.02]$, $[5; 5], [35; 35]$
Excitation rates	Ξ_s, Ξ_e , and Ξ_0	$\text{diag}[1500; 500]$, $5\mathbf{I}_2, 0.5\mathbf{I}_2$
Exponential rates	p_1, q_1, p_2 , and q_2	5, 3, 1, and 3

are respectively strongly activated in two specific ranges of the sliding manifold.

Remark 8: The total control idea is summarized in **Fig. 1**. On one hand, the control algorithm adopts two control layers with three main control gains (\mathbf{K}_0 , \mathbf{K}_1 , and \mathbf{K}_2) to realize the control objective (3). The final control signal (17) is combined from a simple TDE term and various forms of the control error and the sliding manifold synthesized. Thus, proposed control method has less computational burden than previous intelligent controllers which are embedded into fuzzy-logic and neural-network frameworks [7], [8], [13], [14]. On the other hand, the stability of the closed-loop system is theoretically ensured by the robust nonlinear sliding mode design, while the proposed learning laws pro-

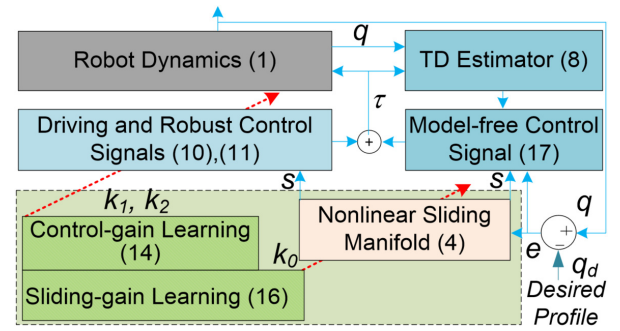


FIGURE 1. Scheme of the proposed controller.

vide the flexibility to user in preserving the desired control performance. According to the inequality (22), the learning (η_0 , η_1 , and η_2) and excitation (Ξ_s , Ξ_e , and Ξ_0) rates can be employed as fixed values depending on physical natures of the control plant.

IV. VALIDATION RESULTS

Performance of the proposed controller was verified both on simulation and extended real-time experiments. Three state-of-the-art controllers, including robust-gain and mass-gain learning TDE controllers (RLTDE vs MLTDE) and a prescribed-performance proportional-derivative (PPPD) controller, were also implemented on the same system as benchmarks for the control-efficiency comparison. Design of the comparative controllers is presented in *Appendix B*. The obtained results are carefully discussed in the following section.

A. SIMULATION RESULTS

The controllers were applied for position-tracking control on simulation of a 2-Degree-of-freedom (DOF) robot, as depicted in **Fig. 2**. Dynamics of the robot are presented in *Appendix C*. Simulation parameters of the controllers and the dynamics are shown in **Tables I** and **II**, respectively.

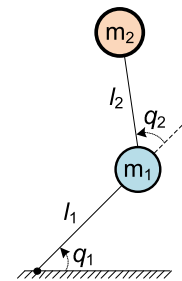


FIGURE 2. A 2-DOF manipulator.

Desired profiles of the robot joint control in the first simulation were sinusoidal signals that are plotted in **Fig. 3**. The control results obtained are presented in **Figs. 4** and **5**.

As shown in **Fig. 4(a)**, transient performances of the RLTDE, MLTDE and proposed controllers for both joints were satisfied the desired convergence rate, while that of the

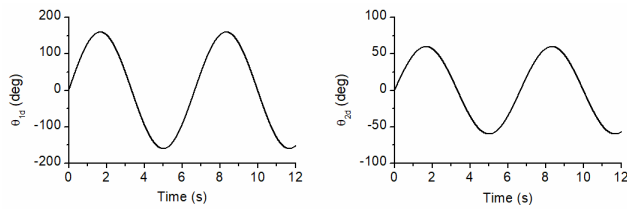
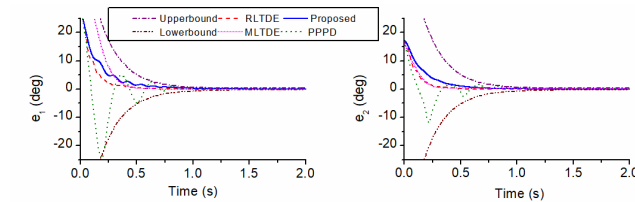
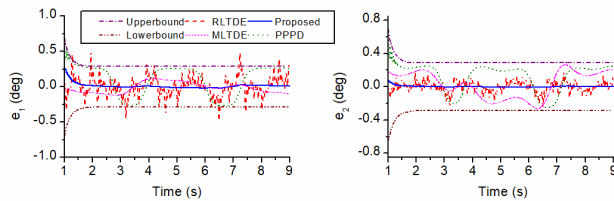


FIGURE 3. Reference signals in the first simulation.



a) Transient error



b) Steady-state error

FIGURE 4. Control errors achieved in the first simulation.

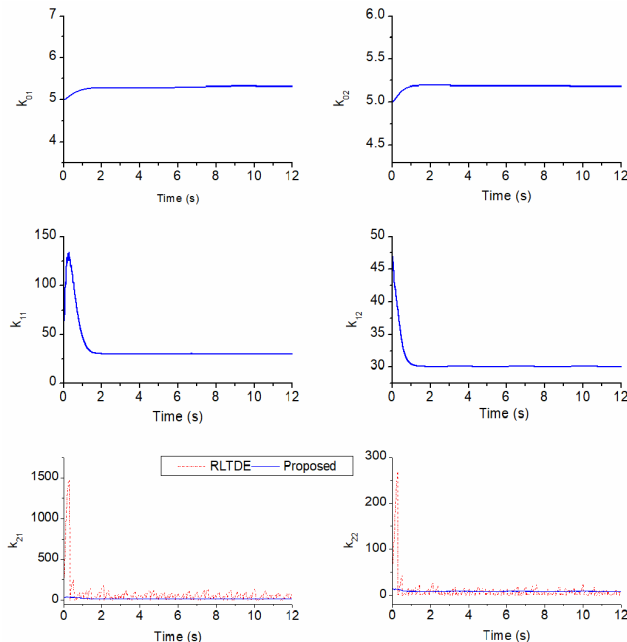


FIGURE 5. Comparative gain learning in the first simulation.

PPPD controller for the first joint was not good as expected. In reality, by using the PPPD control method, the singularity would be originated once the control error was out of the desired range [13], [43], [48]. To attenuate this problem, a sat-

uration function of the extended error (e_i/ρ_i) with 0.001 margin far from the bound were employed.

The steady-state control results shown in Fig. 4(b) indicates that the PPPD performance complied with the given constraints, but it tended to approach the bounds instead of the origin. Minimizing dynamical perturbances by finding the optimal nominal mass gains in the MLTDE control algorithm also resulted in high control accuracy [31]. By possessing the fast updating law for the robust gain, the RLDE controller efficiently suppressed large disturbances, but the closed-loop system was disorganized as approaching the origin [49]. According to the first statement of *Theorem 1* and *Remark 6*, very high control accuracy would be accomplished by the proposed controller. To this end, as depicted in Fig. 5, all control gains were automatically tuned to optimize the control error. Different from the key idea of the RLDE controller which only tuned the robust gain, as seen in learning rule (14), the driving and robust gains of the proposed controller were respectively strongly activated when the sliding manifold was outside and inside of the unit circle. It made the gain variations smoother and did not need to be too large for the high-precision control results.

In the second simulation, these controllers were challenged with a sudden disturbance in a short time at joint 2. Tracking simulation results with respect to the same profiles under the extreme disturbance, as plotted in Fig. 6, are shown in Figs. 7, 8, and 9.

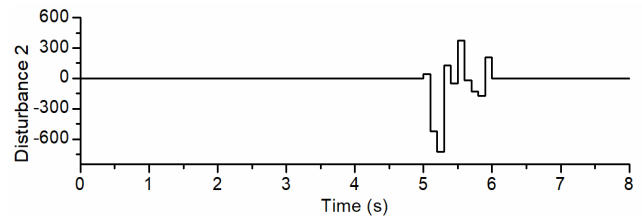


FIGURE 6. Sudden disturbance affected to joint 2.

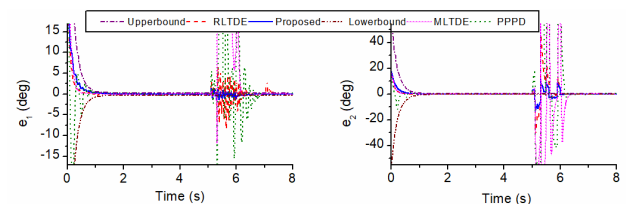


FIGURE 7. Comparative control errors in the second simulation.

Whenever the control error was kicked out of a safety range, recovery ability of the PPPD controller was really poor. This feature is not supported by the PPPD-type control method. Asymptotic control performance was provided by the MLTDE only inside of a certain range of the mass matrix with slow learning rates [31]. Hence, the transient control performance of the MLTDE was under expectation after facing the large disturbance. As seen in Fig. 7, the RLDE could

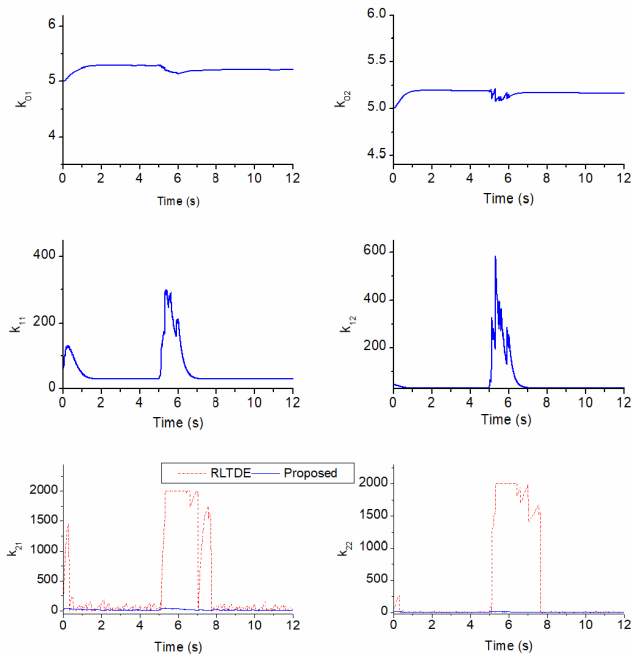


FIGURE 8. Comparative gain variation with the large disturbance.

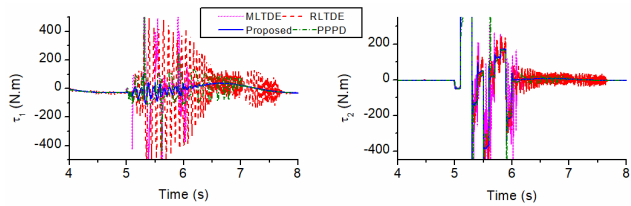


FIGURE 9. Control signals generated to suppress the disturbance in the second simulation.

well deal with this problem thanks to the fast adaptation law (29). As shown in **Fig. 9**, the large robust gain could however generate the ripple or chattering control input. Instead of increasing the robust gain, in the proposed controller, the driving gain played a dominant role in such a case to force the sliding manifold back to zero as fast as possible and the sliding gain worked as a damping term to avoid rebounding problems. The gain behaviors are demonstrated in **Fig. 8**. Influence of the proposed controller against the disturbance is reflexed in **Figs. 7** and **9**.

B. EXPERIMENTAL RESULTS

Real-time experiments were performed to investigate feasibility of the proposed controller. A 6DOF robot was designed and fabricated for the validation. The robot prototype is shown in **Fig. 10**. Industrial motors were employed to actuate the robot joints, and encoders with resolution of 5760ppr were used to measure the joint positions. A compactRIO 9024 controller connecting with digital (NI 9401) and analog (NI 9263) modules was setup as a data acquisition (DAQ)

system. The algorithms were deployed in the Labview environment to control the first joint of the robot.

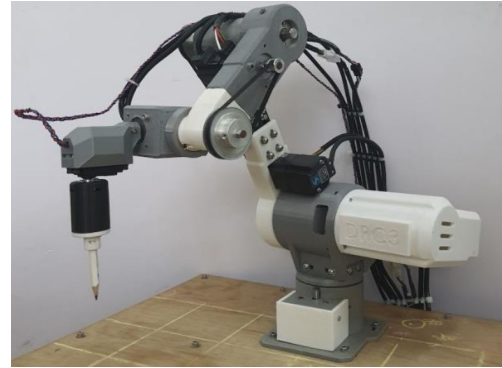


FIGURE 10. The experimental 6DOF robot.

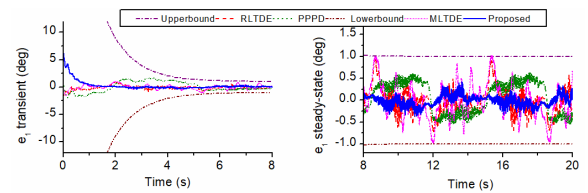


FIGURE 11. Real-time comparative control errors.

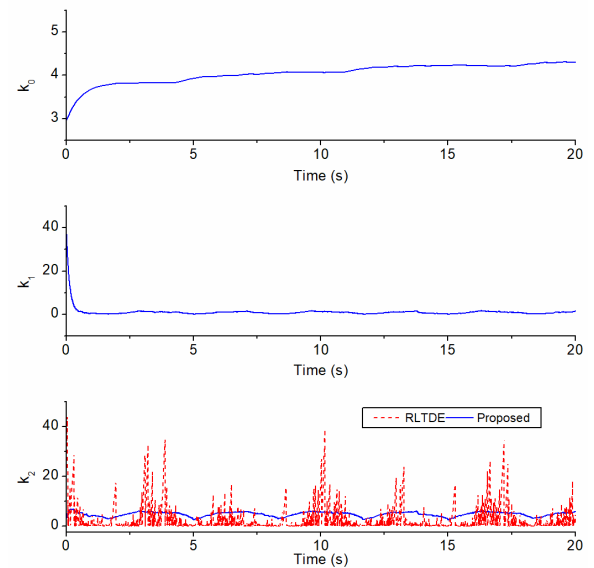


FIGURE 12. Learning ability of the proposed and RLTDE controllers.

The desired profile chosen was: $\theta_{1d} = 30 \sin(0.3\pi t)(\text{deg})$. The control results obtained are shown in **Figs. 11**, **12**, and **13**. Transient control performances of the controllers were not much different due to starting from small initial joint angles. However, interesting information could be observed in the steady-state control errors. The MLTDE provided a learning law to find the optimal nominal mass matrix subjected

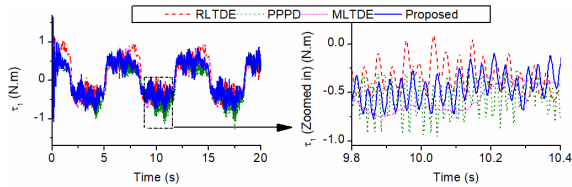


FIGURE 13. Real-time torques generated by the controllers.

to the minimal TDE error. Without employing any robust control signal, the MLTDE only produced an acceptable control error of 0.98 (deg). The control precision could be enhanced by the RLDE controller thanks to the fast robust-gain learning or by the PPPD controller with the prescribed-performance-guarantee mechanism: the RLDE and PPPD errors were 0.75 (deg) and 0.7 (deg), respectively. In fact, the learning ability of the MLTDE and RLDE was only applied to the reaching phase of the sliding mode working principles. With hard sliding procedures, at which the constant sliding gains were employed, good sliding manifolds would result in good control errors. As a solution, adaptation laws of the proposed controller supported two phases of the SMC algorithm. As seen in **Fig. 12**, the driving and robust gains (K_1 and K_2) were strongly activated with respect to large and small ranges of the sliding manifold in the reaching phase, and a soft sliding policy (K_0) was accomplished by the new learning rules (15)-(16). Thus, higher control accuracy of 0.39 (deg) was exhibited by the proposed controller. Control torques generated by the testing controllers are presented in **Fig. 13**. The highest deviation could be observed from the PPPD control signal which was created by logarithmic implication control law to ensure the prescribed bound. The MLTDE used the smoother control torque after the optimal nominal mass matrix was found. To effectively suppress the TDE error, the fast robust-learning law associated with a signum function was employed by the RLDE, but such the robust rule made high-amplitude harmonics in the control signal. The proposed adaptation laws (14)-(16) reveal that the robust-gain (K_2) was mainly busted in the steady-state time of the reaching phase. The high-performance control mission was effectively shared by other control gains in proper control gradation. Hence, as seen in **Fig. 13**, the large-deviation problem would be attenuated by the proposed control method.

As observed in the working progress of the sliding gain (K_0) illustrated in **Fig. 12**, the adaptation rule seemed going to infinite. A long-time experiment with random disturbances was performed to verify this issue. The data obtained are displayed in **Figs. 14** and **15**. To cope with unknown external disturbances, as shown in **Fig. 15**, all the control gains were varied in different ways to maintain the stability of the closed-loop system. Right after the sudden disturbances vanished, the driving and robust gains were quickly reduced to make the system relax while the optimal sliding gains, as noted in **Fig. 14**, was found to result in the high control accuracy. Thus,

TABLE 3. Statistical performance comparison of the controllers from the validation results.

Control Error		Joint 1		Joint 2	
		MA	RMS	MA	RMS
The first simulation	RLTDE	0.4749	0.1417	0.2406	0.0694
	PPPD	0.2715	0.2170	0.2505	0.1890
	MLTDE	0.0847	0.0413	0.2652	0.1776
	Proposed	0.0268	0.0171	0.0086	0.0049
The second simulation	RLTDE	8.3728	1.8853	46.2209	8.5338
	PPPD	36.1909	8.9667	164.64	38.9088
	MLTDE	153.5829	38.5389	139.2691	36.503
	Proposed	1.7547	0.3691	14.1212	3.3696

B) EXPERIMENTAL DATA

Control Error		MA	RMS
The real-time experiment	RLTDE	0.75	0.28
	PPPD	0.7	0.43
	MLTDE	0.98	0.42
	Proposed	0.39	0.13

the stability and feasibility of the proposed controller have been demonstrated clearly in this test.

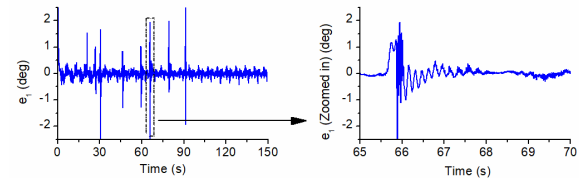


FIGURE 14. A long-time control error of the proposed controller under sudden disturbances.

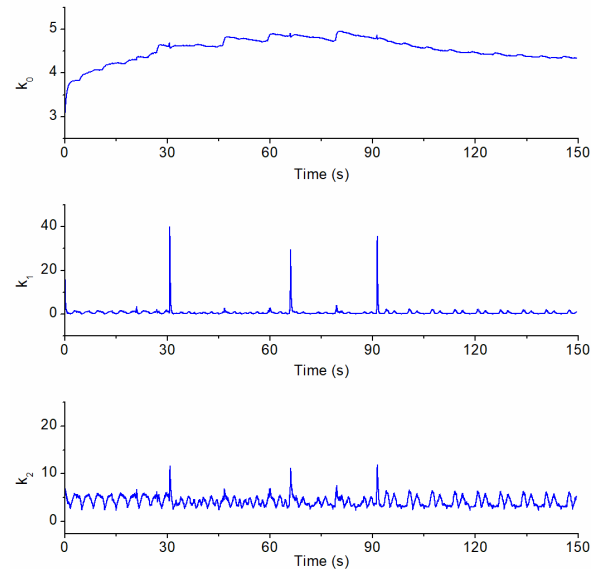


FIGURE 15. An adaptation progress of the control gains in a long-time working under sudden disturbances.

C. DISCUSSION

Table 3 presents the maximum absolute (MA) and root-mean-square (RMS) values of the control errors obtained

by the static computation of the control performances for a manipulated time (5s to 8s). The PPPD controller normally produced the largest RMS control errors as comparing to the others even though its MA errors are in good ranges. The information implies that the uncertain nonlinearities were not treated well in the PPPD algorithm. The statical data also reveal that this issue was efficiently dealt with by the TDE control schemes. Searching the best mass matrix by the MLTDE method could yield the very high control accuracy, but its adjustability was slow in arduous working cases. The RLTDDE possessed a faster adaptation rate but its steady-state control errors were still limited. Both the collected MA and RMS outcomes of the proposed controller always got better than those of the others. To this end, the TDE technique and the multi-level learning rules were combined in a reasonable manner. Hence, promising characteristics of the proposed controller over the previous control methods were confirmed throughout the analytical and testing results.

V. CONCLUSION

In this article, an adaptive robust controller is proposed for high-quality position-tracking control of robot manipulators based on a new nonlinear sliding mode scheme. Effect of the system nonlinearities, uncertainties, and unpredictable disturbances are compensated by a model-free estimator. The control objective is realized using a two-layer control signal. The adaptation ability is integrated into the layers of the control architecture. A new gain-learning law of the high-level control layer is developed to actively stabilize the sliding manifold in a certain bound under a desired convergence rate. Furthermore, another gain-learning law is proposed for the low-level control layer to promptly force the control error back to zero. Asymptotic stability and effectiveness of the closed-loop system are confirmed by Lyapunov-based constraints, intensive simulations, and extended real-time experiments. Ideally choosing the mass matrix would lead to the small-possible TDE error. At that time, the learning burden on the driving and robust gains could be effectively reduced and the convergence rate of the reaching phase could be improved. Theoretical integration of the new whole system is a challenge that could open future research.

APPENDIX A: PROOF OF THEOREM 1

The following Lyapunov function is investigated:

$$L = 0.5s^T \Xi_s s^{p_2/q_2} + 0.5 \sum_{i=1}^2 (\check{\mathbf{k}}_i^T \check{\mathbf{k}}_i) + 0.5e^T \Xi_s \mathbf{K}_0 e \quad (19)$$

The time derivative of the function (1) with noting the control signals (5), (6), (10), (11), and (17) is

$$\begin{aligned} \dot{L} = & (s^{p_2/q_2})^T \Xi_s \check{\mathbf{K}}_0 \dot{\mathbf{K}}_0 (e + e^{p_1/q_1}) + \sum_{i=1}^2 (\check{\mathbf{k}}_i^T \dot{\mathbf{k}}_i) \\ & + (s^{p_2/q_2})^T \Xi_s (\mathbf{v} + \mathbf{M}^{-1} \boldsymbol{\tau} - \ddot{\boldsymbol{\theta}}_d + \mathbf{K}_0 \end{aligned}$$

$$\begin{aligned} & \left(\mathbf{I} + \frac{p_1}{q_1} \text{diag} \left[e^{(p_1-q_1)/q_1} \right] \right) \dot{e} \\ & + e^T \Xi_s \mathbf{K}_0 (s - \mathbf{K}_0 (e + e^{p_1/q_1})) + e^T \Xi_s \check{\mathbf{K}}_0 \dot{\mathbf{K}}_0 e \\ = & (s^{p_2/q_2})^T \Xi_s (\delta - \mathbf{K}_1 s - \mathbf{K}_2 \text{sgn} [s] + \check{\mathbf{K}}_0 \dot{\mathbf{K}}_0 \\ & \times (e + e^{p_1/q_1})) \\ & + (s^{p_2/q_2})^T \Xi_s \check{\mathbf{K}}_0 \left((\text{diag} [\eta_0] \check{\mathbf{K}}_0 + \Xi_0 \text{diag} [|s|]) \right. \\ & \times e - \Xi_e e^{(2p_1-q_1)/q_1} \left. \right) \\ & - (s^{p_2/q_2})^T \Xi_s \check{\mathbf{K}}_0 \\ & \times \left((\Xi_e - \text{diag} [\eta_0] \check{\mathbf{K}}_0 - \Xi_0 \text{diag} [|s|]) e^{p_1/q_1} \right) \\ & + (s^{p_2/q_2})^T \Xi_s \text{diag} [e^2] \check{\mathbf{K}}_0 \Xi_0 \text{diag} [\text{sgn} [s]] \\ & \times |s|^{(q_2-p_2)/q_2} \\ & + \sum_{i=1}^2 (\check{\mathbf{k}}_i^T \dot{\mathbf{k}}_i) - e^T \Xi_s \mathbf{K}_0 \mathbf{K}_0 (e + e^{p_1/q_1}) \\ & + e^T \Xi_s \check{\mathbf{K}}_0 \dot{\mathbf{K}}_0 e \end{aligned} \quad (20)$$

By adopting the separation law (15) and the learning rule (16) of the low-level control gain, the function (20) becomes

$$\begin{aligned} \dot{L} = & (s^{p_2/q_2})^T \Xi_s (\delta - \mathbf{K}_1 s - \mathbf{K}_2 \text{sgn} [s]) \\ & - e^T \Xi_s \check{\mathbf{K}}_0 \text{diag} [\eta_0] \check{\mathbf{K}}_0 e_0 \\ & + \sum_{i=1}^2 (\check{\mathbf{k}}_i^T \dot{\mathbf{k}}_i) - e^T \Xi_s \mathbf{K}_0 \mathbf{K}_0 e - e^T \Xi_s \\ & \times (\mathbf{K}_0 \mathbf{K}_0 - \check{\mathbf{K}}_0 \Xi_e) e^{p_1/q_1} \end{aligned} \quad (21)$$

The function (21) is extended using the error dynamics (4) and the gain-adaptation law (14) as follows:

$$\begin{aligned} \dot{L} = & (s^{p_2/q_2})^T \Xi_s (\delta - \bar{\mathbf{K}}_1 s - \bar{\mathbf{K}}_2 \text{sgn} [s]) \\ & - e^T \Xi_s \check{\mathbf{K}}_0 \text{diag} [\eta_0] \check{\mathbf{K}}_0 e_0 \\ & - \sum_{i=1}^2 (\check{\mathbf{k}}_i^T \text{diag} [\eta_i] \check{\mathbf{k}}_i) - e^T \Xi_s \mathbf{K}_0 \mathbf{K}_0 e \\ & - e^T \Xi_s (\mathbf{K}_0 \mathbf{K}_0 - \check{\mathbf{K}}_0 \Xi_e) e^{p_1/q_1} \\ \leq & -2 \min [\bar{k}_{1 \min}, \eta_{1 \min}, \eta_{2 \min}, \bar{k}_{0 \min}] L \\ & - e^T \Xi_s \check{\mathbf{K}}_0 \text{diag} [\eta_0] \check{\mathbf{K}}_0 e_0 \\ & - (s^{p_2/q_2})^T \Xi_s (\bar{\mathbf{K}}_2 \text{sgn} [s] - \delta) \\ & - e^T \Xi_s (\mathbf{K}_0 \mathbf{K}_0 - \check{\mathbf{K}}_0 \Xi_e) e^{p_1/q_1} \end{aligned} \quad (22)$$

Here, the first statement of Theorem 1 is proven. ■

If the estimation error (δ) does not meet the constraint (12), by noting Holder inequality [47], the time derivative (22) could be rewritten as:

$$\begin{aligned} \dot{L} \leq & -2 \min \left[\left(\bar{k}_{1 \min} - \frac{p_2}{p_2 + q_2} \right), \eta_{1 \min}, \eta_{2 \min}, \bar{k}_{0 \min} \right] L \\ & + \frac{q_2}{p_2 + q_2} \text{trace} \left[\Xi_s (\Delta_\delta - \bar{\mathbf{K}}_2)^{(p_2+q_2)/q_2} \right] \end{aligned}$$

$$\begin{aligned}
\mathbf{M}[\boldsymbol{\theta}] &= \begin{bmatrix} m_2 l_2^2 + 2l_1 l_2 m_2 c_2 + (m_1 + m_2) l_1^2 & m_2 l_2^2 + l_1 l_2 m_2 c_2 \\ m_2 l_2^2 + l_1 l_2 m_2 c_2 & m_2 l_2^2 \end{bmatrix} \\
\mathbf{C}[\boldsymbol{\theta}, \dot{\boldsymbol{\theta}}] \dot{\boldsymbol{\theta}} &= \begin{bmatrix} -m_2 l_1 l_2 s_2 \dot{\theta}_2 (\dot{\theta}_2 + 2\dot{\theta}_1) \\ m_2 l_1 l_2 s_2 \dot{\theta}_1^2 \end{bmatrix} \\
\mathbf{g}[\boldsymbol{\theta}] &= \begin{bmatrix} m_2 l_2 g c_{12} + (m_1 + m_2) l_1 g c_1 \\ m_2 l_2 g c_{12} \end{bmatrix} \\
\mathbf{f}[\dot{\boldsymbol{\theta}}] &= \begin{bmatrix} a_1 \dot{\theta}_1 \\ a_2 \dot{\theta}_2 \end{bmatrix}
\end{aligned} \quad (25)$$

$$\leq -\sigma L + \frac{q_2}{p_2 + q_2} \text{trace} \left[\Xi_s (\Delta_\delta - \bar{\mathbf{K}}_2)^{(p_2 + q_2)/q_2} \right] \quad (23)$$

By applying integral inequalities [23], [46], a steady-state bound of the control error is established:

$$\begin{aligned}
\|\mathbf{e}\|^2 &\leq \frac{2}{\sigma \lambda_{\max}(\Xi_s \mathbf{K}_0)} \frac{q_2}{p_2 + q_2} \text{trace} \\
&\times \left[\Xi_s (\Delta_\delta - \bar{\mathbf{K}}_2)^{(p_2 + q_2)/q_2} \right] \\
&- \frac{1}{\lambda_{\max}(\Xi_s \mathbf{K}_0)} \left((\mathbf{s}^{p_2/q_2})^T \Xi_s \mathbf{s} + \sum_{i=1}^2 (\check{\mathbf{k}}_i^T \check{\mathbf{k}}_i) \right) \\
&- \frac{2}{\lambda_{\max}(\Xi_s \mathbf{K}_0)} \frac{1}{\sigma} \frac{q_2}{p_2 + q_2} \\
&\times \text{trace} \left[\Xi_s (\Delta_\delta - \bar{\mathbf{K}}_2)^{(p_2 + q_2)/q_2} \right] e^{-\sigma t} \\
&+ \frac{2}{\lambda_{\max}(\Xi_s \mathbf{K}_0)} L[0] e^{-\sigma t}
\end{aligned} \quad (24)$$

That leads to the proof of the second statement. ■

APPENDIX B: DESIGN OF COMPARATIVE CONTROLLERS

The prescribed-performance proportional-derivative (PPPD) controller is designed based on a previous work [48]. First, an error-decaying function is chosen as

$$\rho_i = (\rho_{i0} - \rho_{i\infty}) e^{-\gamma t} + \rho_{i\infty} \quad (26)$$

In fact, ρ_i is a bound-guaranteed function of the control error (3) in which ρ_{i0} and $\rho_{i\infty}$ are initial and steady-state bounds, respectively. γ is the convergence rate.

A transformation function is next selected from the control error (3), as follows:

$$\varepsilon_i = \begin{cases} \ln \left(\frac{\kappa + (e_i/\rho_i)}{\kappa - \kappa (e_i/\rho_i)} \right) & e_{i0} \geq 0 \\ \ln \left(\frac{\kappa + \kappa (e_i/\rho_i)}{\kappa - (e_i/\rho_i)} \right) & e_{i0} < 0 \end{cases} \quad \text{with } 0 \leq \kappa \leq 1 \quad (27)$$

where κ is called undershoot of the control error.

A PPPD control signal is then designed using both the control error and the transformation error

$$\boldsymbol{\tau} = -\mathbf{K}_v \dot{\mathbf{e}} - \mathbf{K}_p \mathbf{e} - \mathbf{K}_\varepsilon \frac{\partial \boldsymbol{\varepsilon}}{\partial \mathbf{e}} \mathbf{e} \quad (28)$$

where \mathbf{K}_v , \mathbf{K}_p and \mathbf{K}_ε are positive-definite gain matrices.

The design of the robust-gain-learning TDE (RLTDE) controller is based on another previous work [27], as follows:

$$\begin{cases} \mathbf{s} = \dot{\mathbf{e}} + \mathbf{K}_{c0} \mathbf{e} \\ \boldsymbol{\tau} = \bar{\mathbf{M}} \left(-\ddot{\boldsymbol{\theta}}_{t-T_s} + \bar{\mathbf{M}}^{-1} \boldsymbol{\tau}_{t-T_s} + \ddot{\boldsymbol{\theta}}_d \right. \\ \quad \left. - \mathbf{K}_{c0} \dot{\mathbf{e}} - \mathbf{K}_{c1} \mathbf{s} - \hat{\mathbf{K}}_{c2} \text{sgn}[\mathbf{s}] \right) \\ \dot{\hat{k}}_{c2i} = \begin{cases} \varphi_i \left(\alpha_i^{-1} |s_i[t]| \right)^{\phi[t]} \phi_i[t], & \text{if } \hat{k}_{c2i} > 0 \\ \varphi_i \alpha_i^{-1} |s_i[t]|, & \text{otherwise} \end{cases} \\ \phi_i[t] \text{sgn} \triangleq \lfloor \|\mathbf{s}\|_\infty - \chi \rfloor \end{cases} \quad (29)$$

where \mathbf{K}_{c0} , \mathbf{K}_{c1} and \mathbf{K}_{c2} are sliding, driving and robust gains, respectively; χ is the steady-state sliding surface; and φ_i , α_i are learning rates.

Idea of the mass-gain-learning TDE (MLTDE) controller is delimited as [31]:

$$\begin{cases} \boldsymbol{\tau} = \boldsymbol{\tau}_{t-T_s} + \bar{\mathbf{M}} \left(-\ddot{\boldsymbol{\theta}}_{t-T_s} + \ddot{\boldsymbol{\theta}}_d - 2\mathbf{K}_0 \dot{\mathbf{e}} - \mathbf{K}_0^2 \mathbf{e} \right) \\ i=1..n \begin{cases} \mathbf{s} = \dot{\mathbf{e}} + \mathbf{K}_0 \mathbf{e} \\ \bar{M}_{ii} = -\alpha_{ii} \left(\dot{s}_{ii} s_{ii} + \delta s_{ii}^2 \right), & \text{if } \bar{M}_{ii} > \bar{M}_{ii}^- \\ \bar{M}_{ii} = \bar{M}_{ii}^-, & \text{otherwise} \end{cases} \end{cases} \quad (30)$$

where \mathbf{K}_0 is the sliding gain; \bar{M}_{ii}^- is a defined lower bound; and δ_{ii} , α_{ii} are learning rates.

APPENDIX C: DYNAMICS OF A 2-DOF ROBOT

The robot dynamics depicted in **Fig. 2** are derived as follows [9]:

where θ_i , l_i , m_i , and $a_{i\triangleq|i|1,2}$ are respectively joint angles, link lengths, link masses, and frictional coefficients; g is the gravitational acceleration; and c_i , s_i , and c_{ij} denote $\cos(\theta_i)$, $\sin(\theta_i)$, and $\cos(\theta_i + \theta_j)$, respectively.

REFERENCES

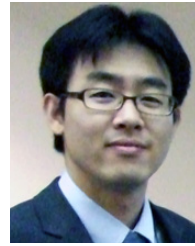
- [1] R. Goel and P. Gupta, "Robotics and industry 4.0," *A Roadmap to Industry 4.0: Smart Production, Sharp Business and Sustainable Development*. Cham, Switzerland: Springer, 2019, pp. 157–169. [Online]. Available: <https://www.springer.com/gp/book/9783030145439>
- [2] N. Shehu and N. Abba, "The role of automation and robotics in buildings for sustainable development," *J. Multidisciplinary Eng. Sci. Technol.*, vol. 6, no. 2, pp. 9557–9560, 2019.
- [3] Y. Park, I. Jo, J. Lee, and J. Bae, "A dual-cable hand exoskeleton system for virtual reality," *Mechatronics*, vol. 49, pp. 177–186, Feb. 2018.
- [4] L. Yang, E. Yu, C.-I. Vong, and L. Zhang, "Discrete-time optimal control of electromagnetic coil systems for generation of dynamic magnetic fields with high accuracy," *IEEE/ASME Trans. Mechatronics*, vol. 24, no. 3, pp. 1208–1219, Jun. 2019.

- [5] Y. Wang, F. Yan, J. Chen, F. Ju, and B. Chen, "A new adaptive time-delay control scheme for cable-driven manipulators," *IEEE Trans. Ind. Informat.*, vol. 15, no. 6, pp. 3469–3481, Jun. 2019.
- [6] J. Baek, W. Kwon, and C. Kang, "A new widely and stably adaptive sliding-mode control with nonsingular terminal sliding variable for robot manipulators," *IEEE Access*, vol. 8, pp. 43443–43454, 2020.
- [7] W. He, Y. Chen, and Z. Yin, "Adaptive neural network control of an uncertain robot with full-state constraints," *IEEE Trans. Cybern.*, vol. 46, no. 3, pp. 620–629, Mar. 2016.
- [8] L. Wu, Q. Yan, and J. Cai, "Neural network-based adaptive learning control for robot manipulators with arbitrary initial errors," *IEEE Access*, vol. 7, pp. 180194–180204, 2019.
- [9] J. J. Craig, *Introduction to Robotics: Mechanics and Control*, 3rd ed. Upper Saddle River, NJ, USA: Prentice-Hall, 2005.
- [10] W. H. Zu, *Virtual Decomposition Control: Toward Hyper Degrees of Freedom Robots*. Berlin, Germany: Springer-Verlag, 2010.
- [11] S. Islam and X. P. Liu, "Robust sliding mode control for robot manipulators," *IEEE Trans. Ind. Electron.*, vol. 58, no. 6, pp. 2444–2453, Jun. 2011.
- [12] W. Kim and C. Chung, "Robust output-feedback control for unknown nonlinear systems with external disturbance," *IET Control Theory Appl.*, vol. 10, no. 2, pp. 173–182, 2016.
- [13] C. P. Bechlioulis and G. A. Rovithakis, "Robust adaptive control of feedback linearizable MIMO nonlinear systems with prescribed performance," *IEEE Trans. Autom. Control*, vol. 53, no. 9, pp. 2090–2099, Oct. 2008.
- [14] M. Wang and A. Yang, "Dynamic learning from adaptive neural control of robot manipulators with prescribed performance," *IEEE Trans. Syst., Man, Cybern. Syst.*, vol. 47, no. 8, pp. 2244–2255, Aug. 2017.
- [15] T. C. Hsia and S. Jung, "A simple alternative to neural network control scheme for robot manipulators," *IEEE Trans. Ind. Electron.*, vol. 42, no. 4, pp. 414–416, Aug. 1995.
- [16] S. Kim and J. Bae, "Force-mode control of rotary series elastic actuators in a lower extremity exoskeleton using model-inverse time delay control," *IEEE/ASME Trans. Mechatron.*, vol. 22, no. 3, pp. 1392–1400, Mar. 2017.
- [17] T. C. S. Hsia, "A new technique for robust control of servo systems," *IEEE Trans. Ind. Electron.*, vol. 36, no. 1, pp. 1–7, Feb. 1989.
- [18] K. Youcef-Toumi and O. Ito, "A time-delay controller for systems with unknown dynamics," *J. Dyn. Syst., Meas., Control*, vol. 112, no. 1, pp. 133–142, 1990.
- [19] Y.-X. Wang, D.-H. Yu, and Y.-B. Kim, "Robust time-delay control for the DC–DC boost converter," *IEEE Trans. Ind. Electron.*, vol. 61, no. 9, pp. 4829–4837, Sep. 2014.
- [20] M. Nikkhah, H. Ashrafiuon, and F. Fahimi, "Robust control of underactuated bipeds using sliding modes," *Robotica*, vol. 25, no. 3, pp. 367–374, May 2007.
- [21] B. Xian, D. M. Dawson, M. S. de Queiroz, and J. Chen, "A continuous asymptotic tracking control strategy for uncertain nonlinear systems," *IEEE Trans. Autom. Control*, vol. 49, no. 7, pp. 1206–1211, Jul. 2004.
- [22] Z. Liu, L. Wang, C. C. L. Chen, X. Zeng, Y. Zhang, and Y. Wang, "Energy-efficiency-based gait control system architecture and algorithm for biped robots," *IEEE Trans. Syst., Man, Cybern., C, Appl. Rev.*, vol. 42, no. 6, pp. 926–933, Nov. 2012.
- [23] J. Yao, Z. Jiao, and D. Ma, "Adaptive robust control of DC motors with extended state observer," *IEEE Trans. Ind. Electron.*, vol. 61, no. 7, pp. 3630–3637, Jul. 2014.
- [24] P. K. Mishra, N. K. Dhar, and N. K. Verma, "Adaptive neural-network control of MIMO nonaffine nonlinear systems with asymmetric time-varying state constraints," *IEEE Trans. Cybern.*, early access, Jul. 11, 2019, doi: 10.1109/TCYB.2019.2923849.
- [25] W. Zhang, J. Bae, and M. Tomizuka, "Modified preview control for a wireless tracking control system with packet loss," *IEEE/ASME Trans. Mechatronics*, vol. 20, no. 1, pp. 299–307, Feb. 2015.
- [26] Y. Zhu, J. Qiao, and L. Guo, "Adaptive sliding mode disturbance observer-based composite control with prescribed performance of space manipulators for target capturing," *IEEE Trans. Ind. Electron.*, vol. 66, no. 3, pp. 1973–1983, Mar. 2019.
- [27] J. Baek, M. Jin, and S. Han, "A new adaptive sliding-mode control scheme for application to robot manipulators," *IEEE Trans. Ind. Electron.*, vol. 63, no. 6, pp. 3628–3637, Jun. 2016.
- [28] Y. Shtessel, M. Taleb, and F. Plestan, "A novel adaptive-gain supertwisting sliding mode controller: Methodology and application," *Automatica*, vol. 48, no. 5, pp. 759–769, May 2012.
- [29] C. Liu, G. Wen, Z. Zhao, and R. Sedaghati, "Neural-network-based sliding-mode control of an uncertain robot using dynamic model approximated switching gain," *IEEE Trans. Cybern.*, early access, Mar. 18, 2020, doi: 10.1109/TCYB.2020.2978003.
- [30] M. Jin, J. Lee, and N. G. Tsagarakis, "Model-free robust adaptive control of humanoid robots with flexible joints," *IEEE Trans. Ind. Electron.*, vol. 64, no. 2, pp. 1706–1715, Feb. 2017.
- [31] J. Lee, P. H. Chang, and M. Jin, "An adaptive gain dynamics for time delay control improves accuracy and robustness to significant payload changes for robots," *IEEE Trans. Ind. Electron.*, vol. 67, no. 4, pp. 3076–3085, Apr. 2020.
- [32] F. Bayat, S. Mobayen, and S. Javadi, "Finite-time tracking control of n th-order chained-form non-holonomic systems in the presence of disturbances," *ISA Trans.*, vol. 63, pp. 78–83, Jul. 2016.
- [33] D. Ashtiani Haghighi and S. Mobayen, "Design of an adaptive super-twisting decoupled terminal sliding mode control scheme for a class of fourth-order systems," *ISA Trans.*, vol. 75, pp. 216–225, Apr. 2018.
- [34] S. Mobayen, "Design of LMI-based sliding mode controller with an exponential policy for a class of underactuated systems," *Complexity*, vol. 21, no. 5, pp. 117–124, May 2016.
- [35] D. X. Ba, H. Yeom, and J. Bae, "A direct robust nonsingular terminal sliding mode controller based on an adaptive time-delay estimator for servomotor rigid robots," *Mechatronics*, vol. 59, pp. 82–94, May 2019.
- [36] M. H. Khooban, T. Niknam, F. Blaabjerg, and M. Dehghani, "Free chattering hybrid sliding mode control for a class of non-linear systems: Electric vehicles as a case study," *IET Sci. Meas. Technol.*, vol. 10, no. 7, pp. 776–785, 2016.
- [37] M. H. Khooban, N. Vafamand, T. Niknam, T. Dragicevic, and F. Blaabjerg, "Model-predictive control based on takagi-sugeno fuzzy model for electrical vehicles delayed model," *IET Electr. Power Appl.*, vol. 11, no. 5, pp. 918–934, May 2017.
- [38] J. Y. Lee, M. Jin, and P. H. Chang, "Variable PID gain tuning method using backstepping control with time-delay estimation and nonlinear damping," *IEEE Trans. Ind. Electron.*, vol. 61, no. 12, pp. 6975–6985, Dec. 2014.
- [39] D. Xuan Ba, H. Yeom, J. Kim, and J. Bae, "Gain-adaptive robust backstepping position control of a BLDC motor system," *IEEE/ASME Trans. Mechatronics*, vol. 23, no. 5, pp. 2470–2481, Oct. 2018.
- [40] Y. Zhu, J. Qiao, and L. Guo, "Adaptive sliding mode disturbance observer-based composite control with prescribed performance of space manipulators for target capturing," *IEEE Trans. Ind. Electron.*, vol. 66, no. 3, pp. 1973–1983, Mar. 2019.
- [41] C. Jing, H. Xu, and X. Niu, "Adaptive sliding mode disturbance rejection control with prescribed performance for robotic manipulators," *ISA Trans.*, vol. 91, pp. 41–51, Aug. 2019.
- [42] C. P. Bechlioulis and G. A. Rovithakis, "Prescribed performance adaptive control for multiinput multioutput affine in the control nonlinear systems," *IEEE Trans. Autom. Control*, vol. 55, no. 5, pp. 1220–1226, Feb. 2010.
- [43] A. K. Kostarigka and G. A. Rovithakis, "Prescribed performance output feedback/observer-free robust adaptive control of uncertain systems using neural networks," *IEEE Trans. Syst., Man, Cybern. B, Cybern.*, vol. 41, no. 6, pp. 1483–1494, Jun. 2011.
- [44] M. Spong and M. Vidyasagar, "Robust linear compensator design for nonlinear robotic control," *IEEE J. Robot. Autom.*, vol. 3, no. 4, pp. 345–351, Aug. 1987.
- [45] M. Jin, J. Lee, P. Hun Chang, and C. Choi, "Practical nonsingular terminal sliding-mode control of robot manipulators for high-accuracy tracking control," *IEEE Trans. Ind. Electron.*, vol. 56, no. 9, pp. 3593–3601, Sep. 2009.
- [46] B. Yao, M. Al-Majed, and M. Tomizuka, "High-performance robust motion control of machine tools: An adaptive robust control approach and comparative experiments," *IEEE/ASME Trans. Mechatronics*, vol. 2, no. 2, pp. 63–76, Jun. 1997.
- [47] Z. Cvetkovski, *Inequalities: Theorems, Techniques, and Selected Problems*. Berlin, Germany: Springer-Verlag, 2012.
- [48] Y. Karayiannidis and Z. Doulgeri, "Model-free robot joint position regulation and tracking with prescribed performance guarantees," *Robot. Auto. Syst.*, vol. 60, no. 2, pp. 214–226, Feb. 2012.
- [49] Y. Su, "Comments on 'A new adaptive sliding-mode control scheme for application to robot manipulators,'" *IEEE Trans. Ind. Electron.*, vol. 67, no. 8, pp. 7116–7120, Aug. 2020.



DANG XUAN BA (Member, IEEE) received the B.S. and M.S. degrees from the Ho Chi Minh City University of Technology, Ho Chi Minh City, Vietnam, in 2008 and 2012, respectively, and the Ph.D. degree from the School of Mechanical Engineering, University of Ulsan, Ulsan, South Korea, in 2016.

He is currently a Lecturer with the Department of Automatic Control, Ho Chi Minh City University of Technology and Education (HCMUTE), Vietnam. He is also the Manager of the Dynamics and Robotic Control (DRC) Laboratory. His research interests include intelligent control, nonlinear control, and modern control theories and their applications.



JOONBUM BAE (Member, IEEE) received the B.S. degree (*summa cum laude*) in mechanical and aerospace engineering from Seoul National University, Seoul, South Korea, in 2006, and the M.S. degree in mechanical engineering, the M.A. degree in statistics, and the Ph.D. degree in mechanical engineering from the University of California at Berkeley, Berkeley, CA, USA, in 2008, 2010, and 2011, respectively.

In 2012, he joined the Department of Mechanical Engineering, Ulsan National Institute of Science and Technology (UNIST), Ulsan, South Korea, where he is currently the Director of the Bio-Robotics and Control (BiRC) Laboratory. He was appointed as a Rising-Star Distinguished Professor of UNIST, in 2018. His current research interests include modeling, design, and control of human-robot interaction systems, soft-robotics, and biologically inspired robot systems. He received Korean Government Minister Awards from the Ministry of Public Safety and Security and the Ministry of Science, ICT and Future Planning, in 2016 and 2017, and the Young Researcher Award from the Korea Robotics Society, in 2015. He was a recipient of a Samsung Scholarship during his Ph.D. studies. He founded a startup named Feel the Same, Inc., in 2017, which develops opt sensor systems.

• • •